INFECTION AND IMMUNITY, May 2010, p. 1915–1923 Vol. 78, No. 5
0019-9567/10/$12.00 doi:10.1128/IAI.01316-09

Intracellular Invasion by *Orientia tsutsugamushi* Is Mediated by Integrin Signaling and Actin Cytoskeleton Rearrangements[▽]

Bon-A Cho,[1] Nam-Hyuk Cho,[1,2]* Seung-Yong Seong,[1] Myung-Sik Choi,[1] and Ik-Sang Kim[1]

Department of Microbiology and Immunology, Seoul National University College of Medicine, Jongno-Gu, Seoul 110-799, Republic of Korea,[1] and Institute of Endemic Disease, Seoul National University Medical Research Center and Bundang Hospital, Jongno-Gu, Seoul 110-799, Republic of Korea[2]

Received 27 November 2009/Returned for modification 3 January 2010/Accepted 3 February 2010

***Orientia tsutsugamushi*, the causative agent of scrub typhus, is an obligate intracellular pathogen. Previously, we reported that the 56-kDa type-specific antigen (TSA56), a major outer membrane protein of *O. tsutsugamushi*, binds to fibronectin and facilitates bacterial entry into the host cell, potentially via an interaction with integrins. Here, we demonstrated that *O. tsutsugamushi* colocalizes with integrin α5β1 and activates integrin signaling effectors, including focal adhesion kinase, Src kinase, and RhoA GTPase, and also recruits signaling adaptors, such as talin and paxillin, to the site of infection. Inhibition of protein tyrosine kinases or RhoA reduced intracellular invasion. We also observed substantial actin reorganization and membrane protrusions at the sites of infection of nonphagocytic host cells. Finally, we identified a region in the extracellular domain of TSA56 that binds to fibronectin. A peptide containing this region was able to significantly reduce bacterial invasion. Taken together, these results clearly indicate that *O. tsutsugamushi* exploits integrin-mediated signaling and the actin cytoskeleton for invasion of eukaryotic host cells.**

Orientia tsutsugamushi, an obligate intracellular organism, is the causative agent of scrub typhus (26), a disease characterized by fever, rash, eschar, pneumonitis, meningitis, and disseminated intravascular coagulation. Scrub typhus can lead to multiorgan failure if it is left untreated, and the mortality rate ranges from 1% to 40% depending on the strain of *O. tsutsugamushi* (29). Scrub typhus is confined geographically to southeastern Asia and is found in many countries in this region, including Korea, Japan, China, and India (26). An estimated 1 billion people in this area are at risk for scrub typhus, and there are an estimated 1 million new cases annually (29). Scrub typhus can be effectively treated with antibiotics, such as doxycycline and chloramphenicol. However, reinfections are common because of the wide variety of antigenically distinct serotypes (11). In addition, decreased efficacy of antibiotic treatments has been reported in several cases (19, 28). Despite the increasing numbers of patients and recurrent outbreaks of scrub typhus in areas where *O. tsutsugamushi* is endemic (16, 19), an effective vaccine has not been developed yet (3).

Bacterial invasion of host cells is mediated primarily by interactions between bacterial surface components and complementary host receptors, which stimulate host signal transduction pathways required for bacterial entry. As an obligate intracellular organism, *O. tsutsugamushi* must be internalized in host cells. However, the molecular basis of intracellular invasion by *O. tsutsugamushi* is poorly characterized. Previously, we reported that *O. tsutsugamushi* uses host fibronectin interactions with one of its outer membrane proteins, the 56-kDa type-specific antigen (TSA56), for internalization (14). Fibronectin can facilitate bacterial entry into host cells, potentially via interactions with integrins. Exploitation of host integrins and subsequent activation of downstream signaling to mediate intracellular invasion have been well documented for various human pathogens (6). In addition, activation or modulation of the host signaling that eventually induces local actin reorganization plays a pivotal role in the entry of many bacterial pathogens into host cells (23, 25).

In the present study, we demonstrated that *O. tsutsugamushi* can activate integrin-mediated signal transduction pathways that induce local actin rearrangements at the infection site in nonphagocytic host cells. Focal adhesion kinase (FAK), Src kinase, and RhoA GTPase are activated by *O. tsutsugamushi* invasion, and the signaling adaptors talin and paxillin are recruited to the site of infection. Inhibitors of protein tyrosine kinases or Rho GTPases significantly reduced bacterial invasion. Finally, we identified a sequence motif in the extracellular domain of TSA56 that binds to fibronectin. Peptides containing this sequence motif blocked bacterial invasion of nonphagocytic host cells. Taken together, these results indicate that *O. tsutsugamushi* exploits integrin-mediated signaling and rearrangements of the actin cytoskeleton for invasion of eukaryotic host cells.

MATERIALS AND METHODS

Cell culture. HeLa cells (ATCC CCL-2; American Type Culture Collection, Manassas, VA), L929 cells (ATCC NCTC929), and FAK$^{-/-}$ (ATCC CRL-2644) and FAK$^{+/+}$ (ATCC CRL-2645) mouse embryonic fibroblast cell lines were maintained in Dulbecco modified Eagle medium (DMEM) (Welgene, Daegu, South Korea) supplemented with 10% heat-inactivated fetal bovine serum (FBS) (Welgene), 100 U/ml penicillin, and 100 μg/ml streptomycin (Gibco BRL, Gaithersburg, MD) at 37°C in the presence of 5% CO_2. Integrin α5-null normal rat intestinal epithelial (RIE1) cells and derived recombinant cell lines stably expressing human integrin α5 (RIE1/α5) or cytoplasmic tailless integrin α5 (RIE1/α5*tl*) were kindly provided by J. W. Lee (Seoul National University, Seoul, South Korea) and were cultured in DMEM containing 5% FBS and 1 mg/ml Geneticin (Gibco BRL) (22).

* Corresponding author. Mailing address: Department of Microbiology and Immunology, Seoul National University College of Medicine, Jongno-Gu, 28 Yongond-Dong, Jongno-Gu, Seoul 110-799, Republic of Korea. Phone: 82-2-740-8392. Fax: 82-2-743-0881. E-mail: chonh@snu.ac.kr.

▽ Published ahead of print on 16 February 2010.

TABLE 1. Amino acid sequences of synthetic peptides derived from the C-terminal region of TSA56[a]

Peptide	Amino acids	Sequence
1	232–261	FAIHNHEQWRSLVVGLAALSNANKPSASPV
2	252–281	NANKPSASPVKVLSDKIIQIYSDIKPFADI
3	282–301	AGINVPDTGLPNSASIEQIQ
4	292–321	PNSASIEQIQSKIQELGDTLEELRDSFDGY
5	312–341	EELRDSFDGYINNAFVNQIHLNFVMPPQAQ
6	334–363	FVMPPQAQQQQGQGQQQQAQATAQEAVAAA
7	353–382	QATAQEAVAAAAVRLLNGSDQIAQLYKDLV
8	373–402	QIAQLYKDLVKLQRHAGIRKAMEKLAAQQE
9	393–422	AMEKLAAQQEEDAKNQGKGDCKQQQGASEK
10	413–442	CKQQQGASEKSKEGKVKETEFDLSMVVGQV

[a] See Fig. 5A.

Preparation of *O. tsutsugamushi*. The Boryong strain of *O. tsutsugamushi* was purified using a modification of a Percoll gradient purification method (14). *O. tsutsugamushi* was propagated in L929 cells. At 3 to 4 days postinfection, infectivity was determined by an indirect immunofluorescence assay (see below). When an infection rate of >90% was obtained, cells were harvested by centrifugation at 6,000 × *g* for 20 min. The cell pellet was resuspended with 6.5 ml of Tris-sucrose (TS) buffer (33 mM Tris-Cl [pH 7.4] and 0.25 M sucrose). Resuspended cells were homogenized with a Polytron homogenizer (Wheaton Inc., Millville, NJ) using 100 strokes and were centrifuged at 200 × *g* for 5 min. The supernatant was mixed with 40% Percoll (Pharmacia Fine Chemicals, Uppsala, Sweden) in TS buffer and centrifuged at 25,000 × *g* for 60 min. The bacterial band was collected and centrifuged at 77,000 × *g* for 30 min. *O. tsutsugamushi* cells were collected and washed three times with TS buffer. The *O. tsutsugamushi* pellet was resuspended in DMEM and stored in liquid nitrogen until it was used. The infectivity titer of the inoculum used was determined as described elsewhere (5), with minor modifications. Infected-cell counting units (ICU) were calculated as follows: [(total number of cells used for infection) × (percentage of infected cells) × (dilution of the *O. tsutsugamushi* suspension)]/100 (5). For infection assays, 2.5×10^6 and 7×10^7 ICU of *O. tsutsugamushi* were used to infect cells cultured in 24-well plates and 100-mm dishes, respectively. UV-inactivated *O. tsutsugamushi* cells were prepared by exposing bacteria to a 30-W UV lamp for 10 min at a distance of 20 cm with gentle shaking.

Antibodies and reagents. Anti-phosphotyrosine monoclonal antibody (MAb) 4G10 and horseradish peroxidase (HRP)-conjugated 4G10 were purchased from Upstate (Waltham, MA). Anti-FAK, anti-pY397 FAK, anti-pY576 FAK, and anti-pY416 Src were purchased from Millipore (Billerica MA). Anti-human integrin α5, anti-human integrin α5β1, anti-talin, anti-paxillin, and anti-N-terminal fibronectin antibodies were purchased from Chemicon Co. (Temecula, CA). Anti-human integrin β1 monoclonal antibody was obtained from Serotec (Raleigh, NC), and anti-RhoA and anti-Cdc42/Rac1 antibodies were obtained from Assay Designs Inc. (Ann Arbor, MI). The secondary antibodies used for immunoblotting were HRP-conjugated anti-mouse or anti-rabbit IgG antibodies (Santa Cruz Biotech Inc., Santa Cruz, CA). Alexa Fluor 488- or Alexa Fluor 594-conjugated anti-human, mouse, and rabbit antibodies used for immunofluorescence assays were purchased from Molecular Probes (Eugene, OR). Alexa Fluor 594-phalloidin and genistein were obtained from Molecular Probes and Sigma-Aldrich (St. Louis, MO), respectively. TSA56 peptides (purity, >90%) (Table 1) were synthesized using a peptide synthesizer (PeptrEX; Peptron Inc., Daejeon, South Korea). Peptides were analyzed by mass spectrometry and high-performance liquid chromatography using C_{18} column chromatography.

Immunofluorescence microscopy. Immunofluorescence techniques were used to visualize *O. tsutsugamushi* (14). Infected monolayers of L929 cells in 24-well tissue culture plates were collected by trypsin treatment at 1 h postinfection. Extracellular or surface-bound bacteria were removed by washing the preparations three times with phosphate-buffered saline (PBS). The infected cells were then fixed in cold 100% methanol for 15 min at 4°C and stained as described previously (5). Cells infected with *O. tsutsugamushi* were incubated with anti-TSA56 (14), followed by Alexa Fluor 488-conjugated rabbit anti-mouse IgG (Molecular Probes). Cells were examined with an Olympus FV1000 confocal laser scanning microscope (Olympus, Tokyo, Japan). Images of cell sections were captured every 200 nm, and all images were analyzed and processed using the Olympus Fluoview software (Olympus). The number of internalized bacteria in 100 randomly selected cells was determined, and the results were expressed as the average ± standard deviation number of intracellular bacteria per cell for three independent experiments.

To assess the association of *O. tsutsugamushi* with host signaling proteins, HeLa cells grown on 12-mm-diameter glass coverslips were incubated with *O. tsutsugamushi* for 30 min at 4°C and then incubated for 10 min or 30 min at 37°C. Samples were rinsed with PBS three times, fixed in PBS containing 4% paraformaldehyde for 15 min at room temperature, and permeabilized in 0.2% Triton X-100 for 15 min. Subsequently, some infected cells were incubated with serum from human patients for 1 h, followed by Alexa Fluor 488-conjugated goat anti-human IgG. The remainder of the infected cells were incubated with antibodies against various host signaling proteins, as indicated below, and then with Alexa Fluor 594-conjugated goat anti-mouse IgG or anti-rabbit IgG. Actin was stained using Alexa Fluor 594-conjugated phalloidin in some experiments. Stained cells were examined with an Olympus FV1000 confocal laser microscope. All images were analyzed and processed using the Olympus Fluoview software or Adobe Photoshop software.

For three-dimensional (3D) image reconstruction, 3D automated scanning was performed by acquiring *x-y* images and stepping through the *z* direction in 200-nm steps. The *x-y* images acquired were loaded into Image Surfer, a 3D image reconstruction freeware program for visualization and analysis of 3D images and data sets (7). The Image Surfer software uses deconvolution techniques to provide volume rendering of image stacks and allows user manipulation of the volume in the *x*, *y*, and *z* dimensions.

Flow cytometry analysis. *O. tsutsugamushi* infectivity with the RIE1 cell line and its derivatives was quantified by flow cytometry. Infected cells were collected by trypsin treatment 24 h postinfection. Surface-bound bacteria were removed by washing preparations three times with PBS. The cells were fixed, permeabilized, and incubated in PBS-2% FBS with anti-TSA56, followed by Alexa Fluor 488-conjugated goat anti-mouse IgG or an isotype control IgG for 30 min on ice. After several washes, samples (10,000 cells/sample) were assayed using a FACScan instrument (Becton Dickinson). The mean fluorescence intensities reflected the infectivities of *O. tsutsugamushi* from stained samples (12).

Immunoblot analysis. HeLa cells were seeded onto 100-mm tissue culture plates in DMEM with 10% FBS and incubated overnight at 37°C. The following day, cells were either not infected or infected with *O. tsutsugamushi*, incubated at 4°C for 30 min, and then quickly shifted to incubation at 37°C in the presence of 5% CO_2 for different times. After collection at each time point, cells were washed three times with ice-cold PBS and then lysed in 0.5% NP-40 lysis buffer (0.5% NP-40, 20 mM Tris [pH 7.4], 150 mM NaCl, complete protease inhibitor cocktail [Sigma-Aldrich], phosphatase inhibitor cocktail [Sigma-Aldrich]). Lysates were centrifuged at 16,000 × *g* for 15 min to pellet insoluble matter. Samples were adjusted so that the protein contents were the same and then boiled in SDS sample buffer. Samples were resolved by SDS-PAGE and transferred to a polyvinylidene difluoride (PVDF) membrane using a Trans-Blot SD semidry transfer cell (Bio-Rad, Hercules, CA). Immunoblots were developed using the Super Signal West Pico chemiluminescent reagent (Pierce Biotechnology, Rockford, IL).

Cellular invasion and association assays. Bacterial invasion and cell association assays were performed as follows. Cells were cultured on 12-mm-diameter glass coverslips in 24-well plates and inoculated with *O. tsutsugamushi*. The plates were spun at 500 × *g* for 5 min to synchronize bacterial contact with the host cell monolayers and then incubated at 37°C for different times. To discriminate between cell surface-associated bacteria and intracellular bacteria, infected cells were stained using the differential immunofluorescence method. First, cells were washed three times with PBS, fixed with 4% paraformaldehyde, and incubated human patient serum for 1 h, and then Alexa Fluor 488-conjugated goat anti-human IgG was used to stain the cell surface-associated bacteria. Next, cells were permeabilized in a 0.2% Triton X-100 solution for 15 min and incubated with an anti-TSA56 MAb, followed by Alexa Fluor 568-conjugated rabbit anti-mouse IgG to stain intracellular bacteria. One hundred cells were randomly selected using an Olympus FV1000 confocal laser microscope and analyzed using the Fluoview software.

Measurement of RhoA and Cdc42/Rac1 activities. RhoA and Cdc42/Rac1 activities were measured by examining RhoA and Cdc42/Rac1 binding to the corresponding effector binding domains fused to glutathione *S*-transferase (GST) in pull-down assays, using the manufacturer's protocol (Assay Designs, Inc.) (31). Briefly, cell lysates were adjusted so that their protein contents were the same, mixed with 400 μg of rhotekin (for RhoA) or PAK1-PBD (for Cdc42 and Rac1), and incubated for 1 h at 4°C. Samples bound to immobilized glutathione beads were washed three times and eluted using SDS sample buffer. As a positive control, a cell lysate was mixed with GTPγ-S and incubated with the GTPase effector binding domains. The GTP-bound GTPases associated with beads were analyzed by immunoblot analysis using anti-RhoA or anti-Cdc42/Rac antibodies.

To inhibit RhoA activity, HeLa cells were treated with the *Clostridium botu-*

linum C3 exoenzyme (2 μg/ml; Sigma-Aldrich) for 18 h in the presence of Lipofectamine 2000 (Invitrogen) as described previously (1) and were subsequently infected with *O. tsutsugamushi*. The bacterial infectivity was assessed at 4 h postinfection by confocal microscopy.

Scanning electron microscopy. For scanning electron microscopy, HeLa cells grown on glass coverslips were infected with *O. tsutsugamushi* for 10 min, washed, and fixed for 20 min with 4% paraformaldehyde in PBS; this was followed by fixation in 2.5% glutaraldehyde in PBS for an additional 72 h at 4°C and then fixation in 1% osmium tetroxide for 1 h. Samples were serially dehydrated with increasing concentrations of ethanol, critical point dried with hexamethyldisilazane, and covered with a gold film by sputter coating for 120 s. The samples were examined using a scanning electron microscope (Hitachi S4700; Hitachi, Japan) at an accelerating voltage of 15 kV.

Peptide fibronectin-binding assay and inhibition assay. Type-specific antigen (TSA) peptides were examined for fibronectin-binding activity by performing an enzyme-linked immunosorbent assay (ELISA) as described previously (13). Briefly, the wells in a 96-well plate were coated overnight with 1.0 μg of peptide (20- or 30-mers). Wells coated with bovine serum albumin (BSA) were used as a negative control. The wells were blocked with 1% BSA for 1 h at 25°C and washed with PBS containing 0.1% (wt/vol) BSA and 0.01% (vol/vol) Tween 20. Fibronectin (1.0 μg; Sigma-Aldrich) was diluted in incubation buffer (PBS containing 0.02% [wt/vol] BSA), added to each well, and incubated for 3 h. Subsequently, wells were washed three times and incubated with a mouse anti-fibronectin antibody. The bound antibody was detected using an anti-mouse IgG-HRP antibody, which was followed by addition of a 3,3′,5,5′-tetramethylbenzidine (TMB) substrate solution (Endogen, Woburn, MA). Binding was quantified by colorimetric detection at 492 nm.

In order to assess the inhibitory effect of TSA peptides on *O. tsutsugamushi* infection, HeLa cells were treated with 50 nM TSA56 peptide or with DMEM alone as a negative control. *O. tsutsugamushi* was added to the HeLa cells and incubated for 3 h. The infected cells were collected by using trypsin treatment, washed three times with PBS to remove surface-bound bacteria, replated on 12-mm coverslips in 24-well plates, and incubated for an additional 24 h. The bacteria replicating in host cells were visualized using an immunofluorescence assay, and the number of bacteria per cell was determined by examining 100 randomly selected cells.

Statistical analyses. Statistical analyses were performed using the Student *t* test with SigmaPlot (Jandel, San Rafael, CA). The data are presented below as means ± standard deviations, and a P value of <0.01 was considered statistically significant.

RESULTS

Colocalization of *O. tsutsugamushi* with integrin α5β1. Since our previous results suggested that there is a potential interaction between *O. tsutsugamushi* and the host integrin α5β1 through formation of a TSA56-fibronectin complex, we first examined whether *O. tsutsugamushi* can interact with integrin α5β1. HeLa cells were observed using confocal microscopy 10 min after infection with *O. tsutsugamushi*. The infected cells were stained using primary antibodies specific for the individual α5 and β1 subunits or for the α5β1 heterodimeric complexes. Analysis of single cross sections from confocal *z* stacks revealed that the α5 and β1 subunits, as well as α5β1 heterodimers, colocalized with cell-associated *O. tsutsugamushi* (Fig. 1A). In order to confirm that the interaction of *O. tsutsugamushi* with the integrins affects bacterial infectivity, we used rat intestinal epithelial cells (RIE1) ectopically overexpressing wild-type or mutant human integrin α5 (RIE1/α5 and RIE1/α5*tl*, respectively) (22). The RIE1/α5*tl* cells express a mutant integrin α5 which lacks the C-terminal 27 amino acids of the cytoplasmic tail and is thus defective in signaling in response to fibronectin binding (15, 22). The surface expression of integrin α5 in the recombinant RIE1 cells was confirmed by fluorescence-activated cell sorting (FACS) analysis (data not shown), as shown previously (15). We measured bacterial infectivity using FACS analysis with these cell lines and found that *O. tsutsugamushi* infected RIE1/α5 cells more efficiently than it infected either RIE1 cells or RIE1/α5*tl* cells (Fig. 1B). The mean fluorescence intensity (MFI), which represented the level of bacterial internalization, was approximately 50% higher for cells overexpressing integrin α5 (RIE1/α5; mean ± standard deviation MFI, 85.94 ± 9.28) than for control RIE1 cells (54.60 ± 6.91) or RIE1/α5*tl* cells (56.91 ± 5.41).

Focal adhesion kinase (FAK) plays a crucial role in integrin-mediated signaling (6, 20). To determine whether FAK also plays a role in *O. tsutsugamushi* entry, we examined bacterial invasion using mouse embryonic fibroblasts (MEFs) derived from either FAK knockout mice or their wild-type littermates. The mean number of bacteria internalized by $FAK^{-/-}$ cells (4.25 bacteria/cell) was 81% less than the mean number of bacteria internalized by $FAK^{+/+}$ cells (21.90 bacteria/cell) (Fig. 1C), whereas there was no significant difference in adherence of the bacteria to the cell surface between the cell lines (data not shown). These results clearly indicate that *O. tsutsugamushi* exploits integrin molecules for invasion of eukaryotic host cells, potentially through activation of integrin α5β1 signal transduction pathways.

Activation of integrin signaling and recruitment of focal adhesion proteins by *O. tsutsugamushi*. Engagement of integrin molecules induces activation of nonreceptor tyrosine kinases, such as FAK or Src family tyrosine kinases, and results in focal adhesion formation (6). Therefore, we examined protein tyrosine phosphorylation in host cells after infection with *O. tsutsugamushi*. HeLa cells were infected with *O. tsutsugamushi*, and changes in the phosphorylation state of host proteins after different times were monitored by immunoblotting with an anti-phosphotyrosine antibody (Fig. 2A, upper panel). *O. tsutsugamushi* induced tyrosine phosphorylation of several host proteins, particularly several proteins in the 120- to 130-kDa range, with a peak of phosphorylation at 10 to 30 min postinfection. FAK (125 kDa) plays a key role in integrin-mediated signaling (6) and is implicated in entry of *O. tsutsugamushi* (Fig. 1C), as well as other intracellular pathogens (17, 25), into nonphagocytic cells. Therefore, activation of FAK was measured using FAK antibodies specific for tyrosine-phosphorylated FAK to test whether FAK is activated upon infection of cells by *O. tsutsugamushi*. We used two anti-phospho-FAK antibodies, which recognize FAK autophosphorylation (pY397) and maximal FAK catalytic activation (pY576) by Src-mediated phosphorylation during integrin-mediated signaling (20). Infection of HeLa cells with *O. tsutsugamushi* induced tyrosine phosphorylation of FAK with a peak at 30 min postinfection (Fig. 2A). In addition, phosphorylation of Src tyrosine kinase (pY416) also gradually increased up to 60 min postinfection. The antibody against pY416 Src often detected double bands representing the active form of Src kinase (32). These results indicate that tyrosine phosphorylation of host proteins, including FAK and Src, is induced during the early stages of *O. tsutsugamushi* entry.

Next, we used confocal microscopy to localize endogenous focal adhesion components in HeLa cells infected with *O. tsutsugamushi*. As shown in Fig. 2B, some of the cell-associated bacteria colocalized with endogenous phospho-FAK (pY397). Talin and paxillin, which are signaling adaptors in focal adhesion, were also strongly concentrated at sites of bacterial entry.

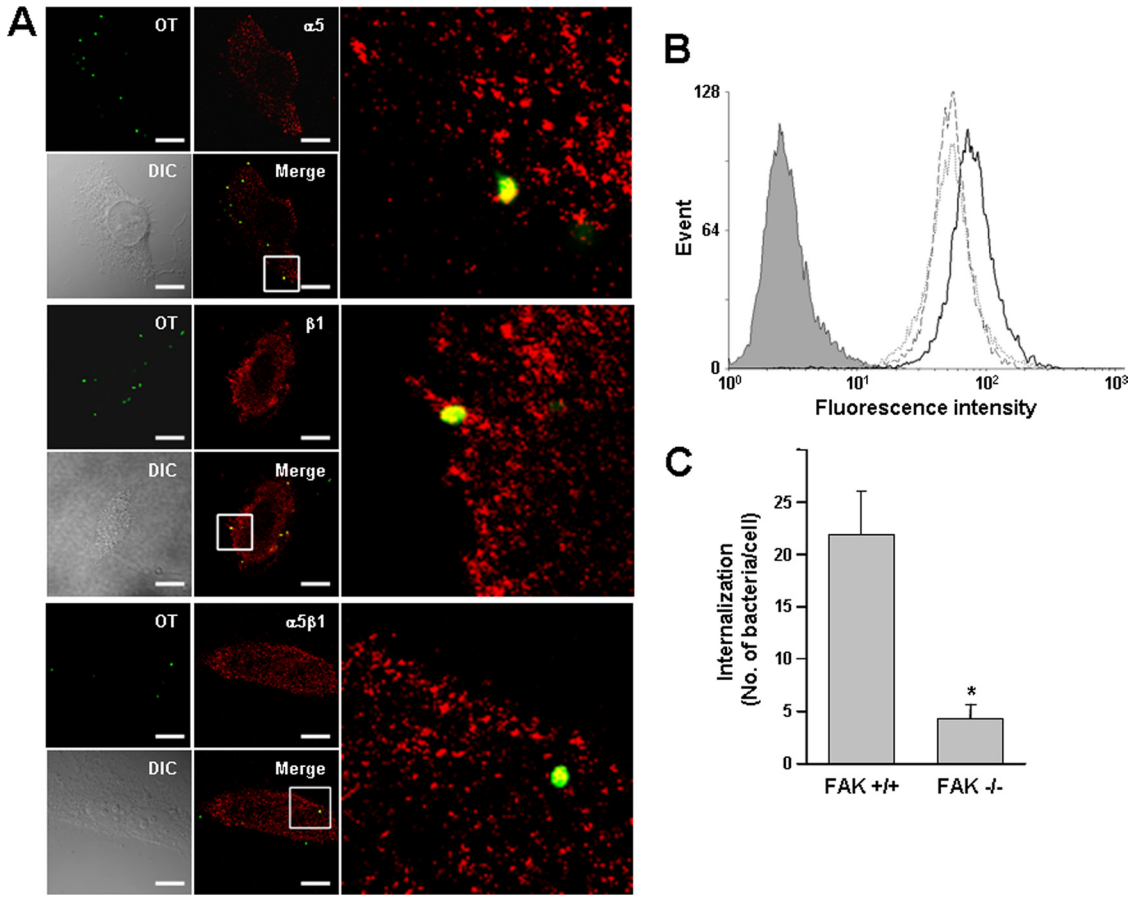

FIG. 1. Colocalization of *O. tsutsugamushi* with cellular integrin α5β1 and involvement of integrin signaling in bacterial entry. (A) Immunofluorescence confocal microscopy of infected HeLa cells showed that *O. tsutsugamushi* (green) colocalizes with integrin α5 and β1 subunits, as well as the integrin α5β1 heterodimeric complexes (red), at 10 min postinfection. The boxes indicate the regions of the merged images that are shown at a higher magnification on the right. OT, *Orientia tsutsugamushi*; DIC, differential interference contrast. Bars, 5 μm. (B) Bacterial infectivity as measured by flow cytometry for control RIE1 cells (dotted line) and recombinant cells overexpressing human integrin α5 (RIE1/α5 cells) (solid line) or mutant integrin α5 lacking the cytoplasmic tail (RIE1/α5*tl* cells) (dashed line). Intracellular bacteria were stained with anti-TSA56 antibody and Alexa Fluor 488-conjugated secondary antibody. The mean fluorescence intensity (MFI) and standard deviation for each group are described in the text. The gray histogram indicates the results for the isotype control. (C) Effect of FAK on bacterial infectivity. Cellular invasion by *O. tsutsugamushi* was evaluated using wild-type ($FAK^{+/+}$) or FAK-null ($FAK^{-/-}$) embryonic fibroblasts by counting the internalized bacteria using confocal microscopy. The average number of internalized bacteria per cell was determined using 100 randomly selected cells. The bars and error bars indicate the means and standard deviations of triplicate experiments. *, $P < 0.01$.

Since not all of the cell-associated *O. tsutsugamushi* colocalized with phospho-FAK, we examined whether viability of the bacteria is required for recruitment and activation of FAK using UV-inactivated bacteria. Although inactivation of *O. tsutsugamushi* had no effect on bacterial adherence, none of the UV-inactivated bacteria were able to recruit phospho-FAK up to 60 min after inoculation. In addition, the levels of FAK phosphorylation did not increase significantly in cells infected with the inactivated bacteria (data not shown). Taken together, these results clearly indicate that recruitment and activation of FAK occur during infection by *O. tsutsugamushi* and that focal adhesion formation is induced at the invasion site.

The involvement of protein tyrosine phosphorylation in *O. tsutsugamushi* invasion of cells was further investigated using genistein, a potent broad-spectrum tyrosine kinase inhibitor. Preincubation of HeLa cells with genistein inhibited *O. tsutsugamushi* invasion in a concentration-dependent manner, but it had no effect on cell surface adherence of the bacteria. These results indicate that tyrosine kinase activity is required for invasion (Fig. 2C).

Activation of the small GTPase RhoA, but not Cdc42 or Rac1, by *O. tsutsugamushi*. Formation of focal adhesions at the site of bacterial entry in host cells is crucial for the uptake of several pathogenic bacteria and has been linked to the activation of small GTPases (25). Here we examined whether *O. tsutsugamushi* can activate small GTPases. Activation of endogenous RhoA, Cdc42, and Rac1 during *O. tsutsugamushi* infection was examined using pull-down assays. HeLa cells infected for different times were lysed and activated. GTPases were recovered based on their binding to a GST fusion protein containing the RhoA-binding domain of rhotekin or the Rac/Cdc42-binding domain of the serine/threonine kinase PAK1. Precipitated GTP-bound forms were subsequently detected by immunoblotting. A time-dependent increase in the level of activated RhoA was observed after *O. tsutsugamushi* infection compared to uninfected controls. The peak levels of activated

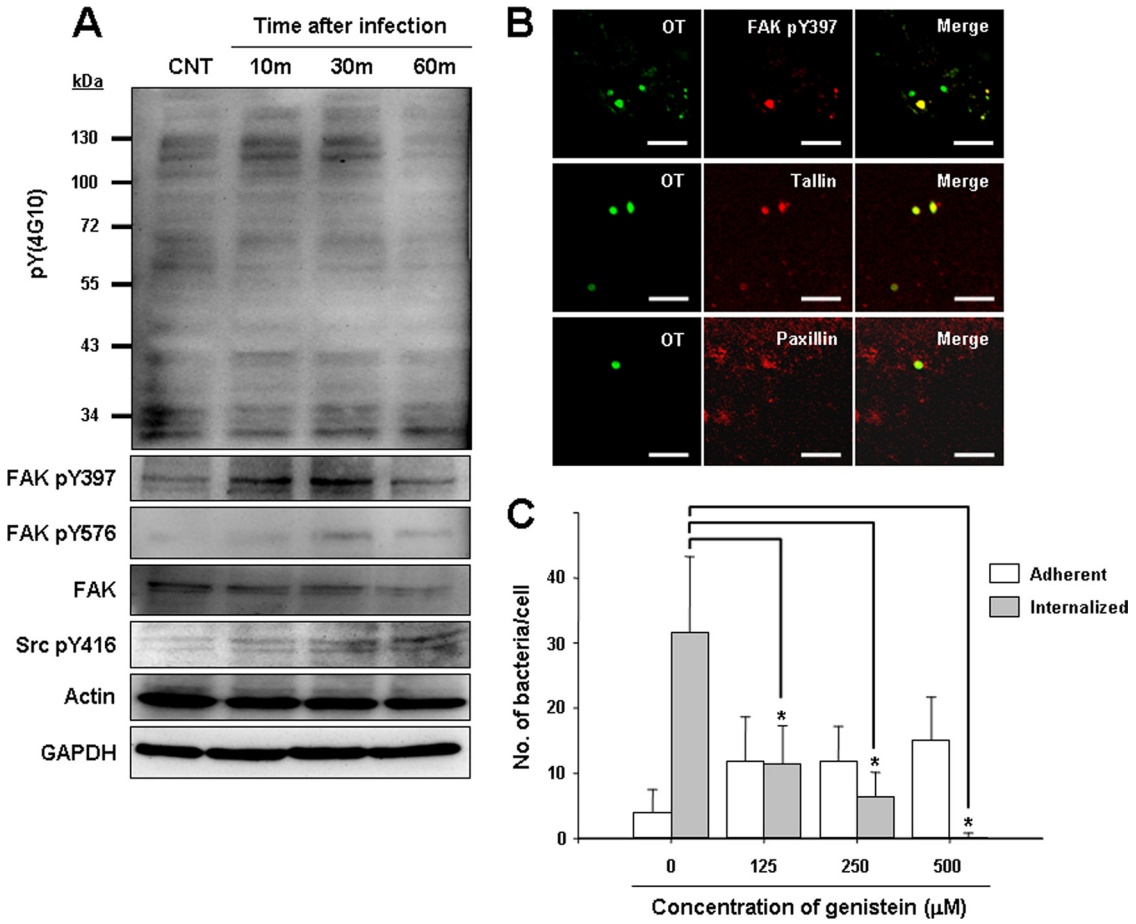

FIG. 2. Activation of integrin signaling by *O. tsutsugamushi* infection. (A) Tyrosine phosphorylation was examined using anti-phosphotyrosine antibody 4G10 and HeLa cells infected for the times indicated (upper panel). Activation of FAK or Src was detected using phospho-specific antibodies (FAK pY397, FAK pY576, and Src pY416). CNT, control; GAPDH, glyceraldehyde-3-phosphate dehydrogenase. (B) Immunofluorescence confocal microscopy revealed that *O. tsutsugamushi* colocalizes with active FAK (FAK pY397), talin, and paxillin by 10 min postinfection. Colocalization was not caused by antibody cross-reactivity as not all adherent bacteria recruited phospho-FAK. OT, *O. tsutsugamushi*. (C) The number of internalized bacteria or adherent bacteria per cell was counted for a random selection of 70 infected cells pretreated with the indicated concentrations of genistein, a protein tyrosine kinase inhibitor. The bars and error bars indicate the means and standard deviations of triplicate experiments. *P* values were determined by comparing untreated samples and treated samples using a two-tailed Student *t* test (*, $P < 0.01$).

RhoA were detected at 30 min postinfection (Fig. 3A). In contrast, Cdc42 and Rac1 were not activated during *O. tsutsugamushi* infection; rather, the levels of active Cdc42 and Rac1 decreased during the early phase of infection.

To further investigate whether activation of RhoA is necessary for intracellular invasion by *O. tsutsugamushi*, HeLa cells were treated with the *C. botulinum* C3 exoenzyme, an inhibitor of the Rho family GTPases (24). C3-catalyzed ribosylation and inactivation of RhoA are at least 100- to 400-fold more efficient than inactivation of Cdc42 or Rac1 (24). Since the C3 exoenzyme lacks a membrane-binding and/or transfer component and thus is not cell permeant, Lipofectamine was used in concert with the C3 exoenzyme to permit toxin entry into the host cells (1). Treatment of HeLa cells with the C3 exoenzyme in the presence of Lipofectamine significantly reduced the efficiency of bacterial internalization by approximately 70% compared to untreated control cells and by 65% compared to cells treated with only Lipofectamine, but it had no significant effect on bacterial adherence (Fig. 3B). Inhibition of *O. tsutsugamushi* invasion by the C3 exoenzyme indicates that a member of the Rho GTPase family has a specific role in bacterial internalization.

Actin cytoskeletal and membrane rearrangements at the site of *O. tsutsugamushi* invasion. Activation of integrin signaling and subsequent activation of FAK and Rho GTPases induce rearrangements of the actin cytoskeleton, which may be necessary for bacterial entry into nonphagocytic host cells. The effect of bacterial adherence on the host cell cytoskeleton was visualized using HeLa cells infected with *O. tsutsugamushi* for different times. As shown in Fig. 4A, some of the adherent bacteria induced actin cytoskeleton rearrangements by 10 min postinfection, suggesting that recruitment of actin is involved in bacterial uptake. The actin rearrangements appeared to be specific to the invading bacteria. When we reconstructed the confocal images using a 3D format, the bacteria that induced actin rearrangements were completely internalized by 30 min postinfection (Fig. 4A, right panel).

Since it appeared that *O. tsutsugamushi* could induce the

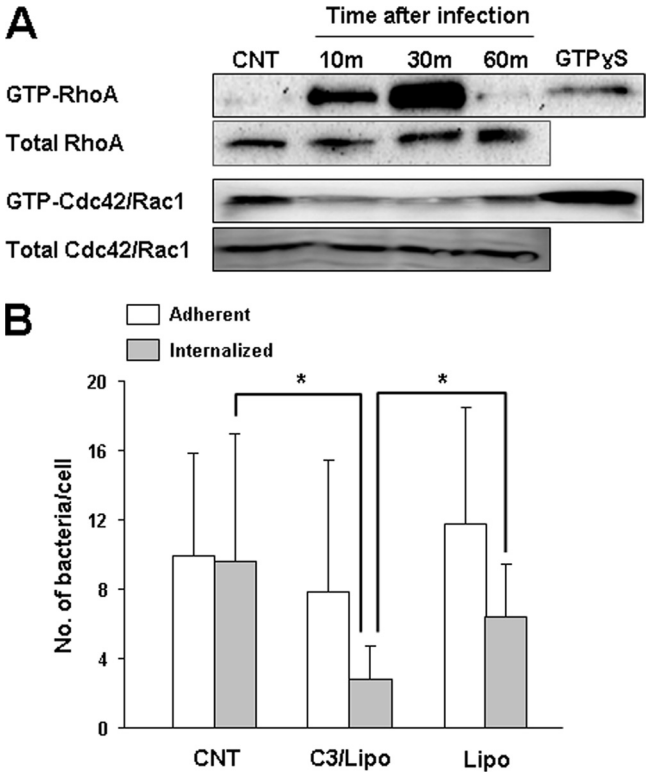

FIG. 3. Activation of RhoA GTPase by *O. tsutsugamushi* infection. (A) Activation of small GTPases was examined by performing GST pull-down assays using rhotekin (for RhoA) or PAK1-PBD (for Cdc42 and Rac1) fusion proteins as described in Materials and Methods. RhoA was activated upon bacterial infection, but Cdc42/Rac1 was not activated. The GTPase active forms bound to GTPγ-S were used as positive controls. CNT, control. (B) Inhibition of intracellular invasion of *O. tsutsugamushi* by *C. botulinum* C3 exoenzyme, an inhibitor of RhoA family GTPases. HeLa cells were treated with the exoenzyme in the presence of Lipofectamine (C3/Lipo) or in the presence of only Lipofectamine (Lipo). *P* values were determined using a two-tailed Student *t* test (*, $P < 0.01$).

formation of membrane protrusions around bacteria, as shown by 3D images obtained at 10 min postinfection, we examined infected HeLa cells by using scanning electron microscopy. Many of the cell-associated *O. tsutsugamushi* bacteria appeared to be entangled in microvilli, which are present in great abundance on the surface of cells, suggesting that the membrane rearrangements have a role in bacterial internalization (Fig. 4B).

Inhibition of *O. tsutsugamushi* invasion by a fibronectin-binding fragment of TSA56. Previously, we found that the C-terminal region (amino acids 243 to 349) of TSA56 binds fibronectin and reduces the intracellular invasion of *O. tsutsugamushi*, potentially by competitive inhibition of the bacterial interaction with fibronectin (14). To further characterize the fibronectin-binding domain of TSA56 and examine its inhibitory effects on bacterial invasion, overlapping peptides corresponding to the C-terminal region of TSA56 (20- or 30-mers with a 10-amino-acid overlap) were synthesized (Fig. 5A). The amino acid sequence of each peptide is shown in Table 1. Maximum fibronectin-binding activity was exhibited by TSA56 peptides extending from amino acid 312 to amino acid 341 (peptide 5) and from amino acid 292 to amino acid 321 (peptide 4) as determined by ELISA (Fig. 5B, red circles and error bars). An additional experiment was performed to determine whether the TSA56 peptides were capable of reducing *O. tsutsugamushi* invasion of HeLa cells. Even though several peptides statistically significantly reduced bacterial internalization, peptide 5, which exhibited the maximum fibronectin-binding capacity, was the most efficient peptide for blocking bacterial invasion (Fig. 5B, bar graph, and 5C). Collectively, amino acid residues 312 to 341 of TSA56 may mediate the interaction with fibronectin, which facilitates intracellular invasion by *O. tsutsugamushi* (14), and the corresponding peptide is sufficient to reduce bacterial entry into host cells, potentially by blocking the TSA56-fibronectin interaction. These results suggest that competitive inhibition of bacterium-fibronectin binding may eventually abrogate the integrin-mediated signaling that is required for bacterial invasion.

DISCUSSION

Establishment of a successful infection and intracellular growth of *O. tsutsugamushi* require efficient intracellular invasion of host cells. However, the signal transduction events leading to intracellular invasion by *O. tsutsugamushi* have not been clearly delineated. Our current results are the first results that clearly demonstrate that *O. tsutsugamushi* exploits host integrin signaling pathways to mediate rearrangements of the actin cytoskeleton for entry into nonphagocytic host cells. Engagement of integrin α5β1 molecules on the host cell surface, which is crucial for bacterial entry, plays a role in the early steps of the invasion process by activating protein tyrosine kinases, such as FAK and Src. Subsequent activation of RhoA and local rearrangement of the actin cytoskeleton at the site of infection may promote bacterial uptake. Based on our previous results (14), the interaction of TSA56, a major outer membrane protein of *O. tsutsugamushi*, with fibronectin may mediate engagement of integrin receptors. The inhibition of bacterial invasion by a C-terminal peptide from TSA56 supports the hypothesis that formation of a TSA56-fibronectin complex may be involved in the activation of integrin signaling (Fig. 5). Further investigation of whether the TSA56-fibronectin complex can directly induce focal adhesion formation at the site of bacterial entry is needed.

Exploitation of integrin signaling is a common strategy used by invasive pathogens, such as *Yersinia* (9), *Staphylococcus aureus* (10), *Streptococcus pyogenes* (21), and *Neisseria* (27), to mediate their uptake by nonphagocytic host cells (25). A *Yersinia pseudotuberculosis* invasion protein (9) and the *Streptococcus* antigen I/II, SspA, and SspB proteins (21) promote bacterial entry by direct binding to host integrins, whereas the fibronectin-binding proteins (FnBPs) of *S. aureus* (10) and the Opc protein of *Neisseria meningitidis* (27) enable these pathogens to bind fibronectin and thereby mediate interactions with integrins to trigger internalization into host cells. *O. tsutsugamushi* appears to use the latter strategy to interact with host integrins, as described previously (14). After integrin engagement, signaling molecules at the inner surface of the plasma membrane that act as integrators of responses to extracellular stimuli are activated. FAK is one such effector and links the stimuli to the actin cytoskeleton (25). FAK colocalizes with

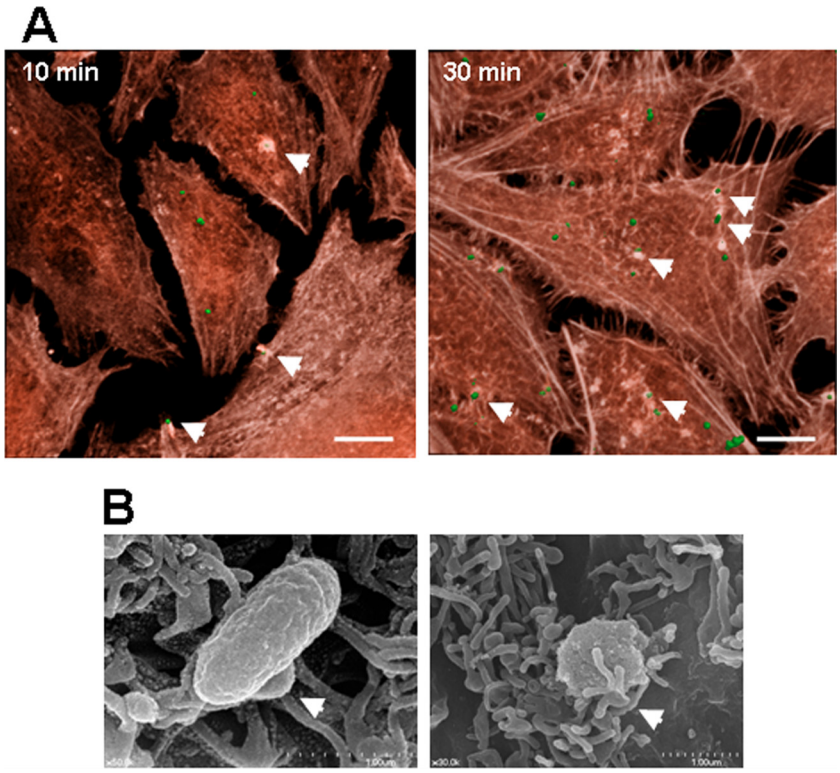

FIG. 4. Induction of local actin reorganization and membrane protrusion at the site of *O. tsutsugamushi* infection. (A) HeLa cells infected with *O. tsutsugamushi* for 10 min or 30 min were stained with Alexa Fluor 594-conjugated phalloidin to detect actin filaments (red). Some of the cell-associated bacteria (arrowheads) induced local rearrangements of the actin cytoskeleton surrounding *O. tsutsugamushi* (green). Bars, 10 μm. (B) Scanning electron microscopy examination of the surface interaction of *O. tsutsugamushi* with HeLa cells. HeLa cells on glass coverslips were infected for 10 min and processed for scanning electron microscopy. The arrowheads indicate membrane protrusions surrounding the cell-associated bacteria.

integrins at focal adhesion points and, upon activation, associates with Src tyrosine kinases, which then promote tyrosine phosphorylation of various substrates, resulting in extensive cytoskeletal reorganization. Therefore, it is not surprising that various microbial pathogens exploit integrin-induced cytoskeletal reorganization to achieve actin-driven uptake (25). *O. tsutsugamushi* activated and recruited FAK to the infection site (Fig. 2), and internalization of this pathogen was severely impaired in FAK-null fibroblasts (Fig. 1C) or by treatment of cells with a tyrosine kinase inhibitor (Fig. 2C). Furthermore, extensive actin reorganization and membrane ruffling in the region surrounding the invading *O. tsutsugamushi* cells were induced within 10 min after infection (Fig. 4). Bacteria that were able to induce reorganization of the actin cytoskeleton were internalized efficiently, as shown by confocal microscopy.

In the context of integrin-dependent uptake, signaling to the actin cytoskeleton involves either RhoA or Rac1 (and sometimes Cdc42) activity (6). Here, we found that *O. tsutsugamushi* activated the RhoA GTPase but not Cdc42/Rac1 (Fig. 3A) and that an inhibitor of RhoA, the *C. botulinum* C3 exoenzyme, reduced bacterial entry into host cells (Fig. 3B). Although the mechanism by which integrin signaling is linked to the activation of RhoA is currently unknown, it is interesting that different isotypes of integrin β-chains are involved in the activation of specific small GTPases (8, 30). Despite the *O. tsutsugamushi* colocalization with integrin β1 observed by confocal microscopy (Fig. 1A), determination of the precise mechanism by which *O. tsutsugamushi* preferentially activates the RhoA GTPase downstream of integrin ligation is a fascinating challenge for future studies. Recently, it has been reported that multiple membrane proteins of *Rickettsia conorii*, a close relative of *Orientia*, are involved in bacterial adherence to, and invasion of, mammalian cells (2, 18). These observations suggest that multiple "surface cell antigen" (*sca*) genes may work in concert to interact with target host cells. At least 17 predicted *sca* genes have been identified in the genomes of *Rickettsia* sp. strains so far (2). Previously, we reported that 6 *sca* genes were found in the genome of *O. tsutsugamushi* (4). Therefore, membrane proteins other than TSA56 may interact with other receptor-ligand pairs to trigger the observed downstream signaling events, involving recruitment of host endocytic machinery components and specific activation of them, that ultimately lead to the extensive actin reorganization required for pathogen entry.

Finally, we searched for specific amino acid motifs in TSA56 that mediate the interaction with fibronectin, which could provide a mechanism for bacteria to bind host integrins for invasion. Previously, we showed that antigenic domain III (AD III) and the adjacent C-terminal region of TSA56 form the putative fibronectin-binding domain (Fig. 5A) and that this peptide fragment could inhibit bacterial invasion. However, we were unable to detect any conserved repeat motifs or sequences that

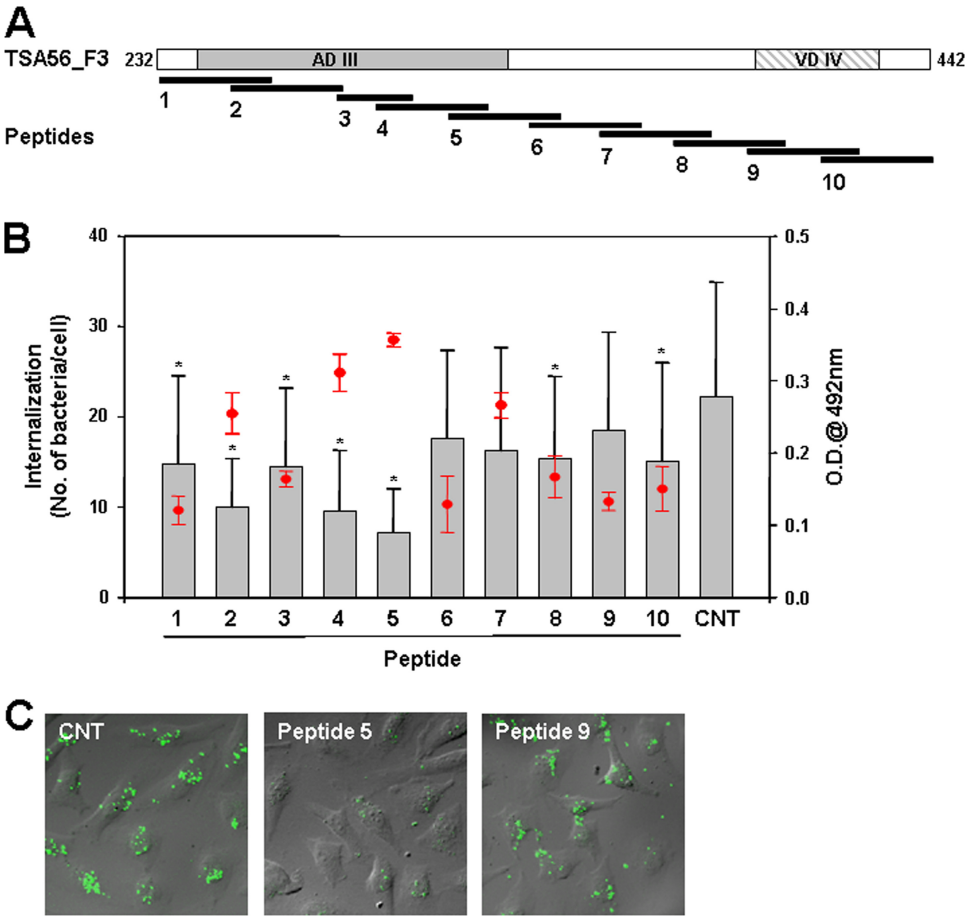

FIG. 5. Fibronectin binding to TSA56 peptides and peptide inhibition of bacterial invasion. (A) Schematic diagram of the overlapping peptides covering the C-terminal region (amino acids 232 to 442) of TSA56. Each peptide overlaps the next peptide by 10 amino acids, except for peptide 3, which contains only 20 amino acids (Table 1). (B) Fibronectin-binding ability of TSA56 peptides (1 μg per well) as measured by ELISA. Bound fibronectin was detected as described in Materials and Methods, and the data shown are the values after subtraction of binding by negative control BSA-coated wells. The means ± standard deviations for fibronectin-TSA56 peptide binding are indicated by red circles and error bars. For the bacterial invasion blocking assay, HeLa cells were incubated with *O. tsutsugamushi* in the presence of each peptide. At 3 h postinfection, adherent bacteria were removed by trypsin treatment, and infected cells were then incubated for an additional 24 h. The number of internalized bacteria per cell was determined using confocal microscopy by examining 100 randomly selected cells per sample; the bars and error bars indicate the means and standard deviations of triplicate experiments. *P* values were determined using a two-tailed Student *t* test (*, $P < 0.01$). CNT, control; O.D.@ 492 nm, optical density at 492 nm. (C) Representative micrographs demonstrating the inhibitory effects of the TSA56 peptides. Internalized bacteria were stained with the anti-TSA56 antibody, followed by Alexa Fluor 488-conjugated anti-mouse IgG (green), and the fluorescence images and phase-contrast images of HeLa cells were overlaid.

have been reported for other fibronectin-binding domains (14). Here, we found that a peptide corresponding to amino acids 312 to 341 of TSA56 interacted with fibronectin and blocked bacterial invasion when it was added to the infection medium (Fig. 5). These results further support the hypothesis that interference with the *O. tsutsugamushi* fibronectin-mediated interaction with host cell integrins could severely impair bacterial entry into host cells. Since the sequence motif of TSA56 is highly conserved across *O. tsutsugamushi* strains (data not shown), this motif could be an attractive target for the development of vaccines and therapeutics for treatment of scrub typhus.

ACKNOWLEDGMENT

This study was supported by grant A090053 from the Korea Healthcare Technology R&D Project, Ministry for Health, Welfare & Family Affairs, Republic of Korea.

REFERENCES

1. **Burnham, C. A., S. E. Shokoples, and G. J. Tyrrell.** 2007. Rac1, RhoA, and Cdc42 participate in HeLa cell invasion by group B streptococcus. FEMS Microbiol. Lett. **272:**8–14.
2. **Cardwell, M. M., and J. J. Martinez.** 2009. The Sca2 autotransporter protein from Rickettsia conorii is sufficient to mediate adherence to and invasion of cultured mammalian cells. Infect. Immun. **77:**5272–5280.
3. **Chattopadhyay, S., and A. L. Richards.** 2007. Scrub typhus vaccines: past history and recent developments. Hum. Vaccines **3:**73–80.
4. **Cho, N. H., H. R. Kim, J. H. Lee, S. Y. Kim, J. Kim, S. Cha, S. Y. Kim, A. C. Darby, H. H. Fuxelius, J. Yin, J. H. Kim, J. Kim, S. J. Lee, Y. S. Koh, W. J. Jang, K. H. Park, S. G. Andersson, M. S. Choi, and I. S. Kim.** 2007. The Orientia tsutsugamushi genome reveals massive proliferation of conjugative type IV secretion system and host-cell interaction genes. Proc. Natl. Acad. Sci. U. S. A. **104:**7981–7986.
5. **Cho, N. H., S. Y. Seong, M. S. Huh, T. H. Han, Y. S. Koh, M. S. Choi, and I. S. Kim.** 2000. Expression of chemokine genes in murine macrophages infected with Orientia tsutsugamushi. Infect. Immun. **68:**594–602.
6. **Dupuy, A. G., and E. Caron.** 2008. Integrin-dependent phagocytosis: spreading from microadhesion to new concepts. J. Cell Sci. **121:**1773–1783.
7. **Feng, D., D. Marshburn, D. Jen, R. J. Weinberg, R. M. Taylor II, and A.**

Burette. 2007. Stepping into the third dimension. J. Neurosci. **27:**12757–12760.
8. **Gustavsson, A., M. Yuan, and M. Fallman.** 2004. Temporal dissection of beta1-integrin signaling indicates a role for p130Cas-Crk in filopodia formation. J. Biol. Chem. **279:**22893–22901.
9. **Hamburger, Z. A., M. S. Brown, R. R. Isberg, and P. J. Bjorkman.** 1999. Crystal structure of invasin: a bacterial integrin-binding protein. Science **286:**291–295.
10. **Hauck, C. R., and K. Ohlsen.** 2006. Sticky connections: extracellular matrix protein recognition and integrin-mediated cellular invasion by Staphylococcus aureus. Curr. Opin. Microbiol. **9:**5–11.
11. **Kelly, D. J., P. A. Fuerst, W. M. Ching, and A. L. Richards.** 2009. Scrub typhus: the geographic distribution of phenotypic and genotypic variants of Orientia tsutsugamushi. Clin. Infect. Dis. **48**(Suppl. 3)**:**S203–S230.
12. **Kim, M. J., M. K. Kim, and J. S. Kang.** 2007. Improved antibiotic susceptibility test of Orientia tsutsugamushi by flow cytometry using monoclonal antibody. J. Korean Med. Sci. **22:**1–6.
13. **Konkel, M. E., J. E. Christensen, A. M. Keech, M. R. Monteville, J. D. Klena, and S. G. Garvis.** 2005. Identification of a fibronectin-binding domain within the Campylobacter jejuni CadF protein. Mol. Microbiol. **57:**1022–1035.
14. **Lee, J. H., N. H. Cho, S. Y. Kim, S. Y. Bang, H. Chu, M. S. Choi, and I. S. Kim.** 2008. Fibronectin facilitates the invasion of Orientia tsutsugamushi into host cells through interaction with a 56-kDa type-specific antigen. J. Infect. Dis. **198:**250–257.
15. **Lee, J. W., and R. L. Juliano.** 2000. Alpha5beta1 integrin protects intestinal epithelial cells from apoptosis through a phosphatidylinositol 3-kinase and protein kinase B-dependent pathway. Mol. Biol. Cell **11:**1973–1987.
16. **Liu, Y. X., D. Feng, J. J. Suo, Y. B. Xing, G. Liu, L. H. Liu, H. J. Xiao, N. Jia, Y. Gao, H. Yang, S. Q. Zuo, P. H. Zhang, Z. T. Zhao, J. S. Min, P. T. Feng, S. B. Ma, S. Liang, and W. C. Cao.** 2009. Clinical characteristics of the autumn-winter type scrub typhus cases in south of Shandong province, northern China. BMC Infect. Dis. **9:**82.
17. **Martinez, J. J., and P. Cossart.** 2004. Early signaling events involved in the entry of Rickettsia conorii into mammalian cells. J. Cell Sci. **117:**5097–5106.
18. **Martinez, J. J., S. Seveau, E. Veiga, S. Matsuyama, and P. Cossart.** 2005. Ku70, a component of DNA-dependent protein kinase, is a mammalian receptor for Rickettsia conorii. Cell **123:**1013–1023.
19. **Mathai, E., J. M. Rolain, G. M. Verghese, O. C. Abraham, D. Mathai, M. Mathai, and D. Raoult.** 2003. Outbreak of scrub typhus in southern India during the cooler months. Ann. N. Y. Acad. Sci. **990:**359–364.
20. **Mitra, S. K., and D. D. Schlaepfer.** 2006. Integrin-regulated FAK-Src signaling in normal and cancer cells. Curr. Opin. Cell Biol. **18:**516–523.
21. **Nobbs, A. H., B. H. Shearer, M. Drobni, M. A. Jepson, and H. F. Jenkinson.** 2007. Adherence and internalization of Streptococcus gordonii by epithelial cells involves beta1 integrin recognition by SspA and SspB (antigen I/II family) polypeptides. Cell. Microbiol. **9:**65–83.
22. **Oh, M. A., E. S. Kang, S. A. Lee, E. O. Lee, Y. B. Kim, S. H. Kim, and J. W. Lee.** 2007. PKCdelta and cofilin activation affects peripheral actin reorganization and cell-cell contact in cells expressing integrin alpha5 but not its tailless mutant. J. Cell Sci. **120:**2717–2730.
23. **Pizarro-Cerda, J., and P. Cossart.** 2006. Bacterial adhesion and entry into host cells. Cell **124:**715–727.
24. **Ridley, A. J., and A. Hall.** 1992. The small GTP-binding protein rho regulates the assembly of focal adhesions and actin stress fibers in response to growth factors. Cell **70:**389–399.
25. **Rottner, K., T. E. Stradal, and J. Wehland.** 2005. Bacteria-host-cell interactions at the plasma membrane: stories on actin cytoskeleton subversion. Dev. Cell **9:**3–17.
26. **Seong, S. Y., M. S. Choi, and I. S. Kim.** 2001. Orientia tsutsugamushi infection: overview and immune responses. Microbes Infect. **3:**11–21.
27. **Unkmeir, A., K. Latsch, G. Dietrich, E. Wintermeyer, B. Schinke, S. Schwender, K. S. Kim, M. Eigenthaler, and M. Frosch.** 2002. Fibronectin mediates Opc-dependent internalization of Neisseria meningitidis in human brain microvascular endothelial cells. Mol. Microbiol. **46:**933–946.
28. **Watt, G., C. Chouriyagune, R. Ruangweerayud, P. Watcharapichat, D. Phulsuksombati, K. Jongsakul, P. Teja-Isavadharm, D. Bhodhidatta, K. D. Corcoran, G. A. Dasch, and D. Strickman.** 1996. Scrub typhus infections poorly responsive to antibiotics in northern Thailand. Lancet **348:**86–89.
29. **Watt, G., and P. Parola.** 2003. Scrub typhus and tropical rickettsioses. Curr. Opin. Infect. Dis. **16:**429–436.
30. **Wiedemann, A., J. C. Patel, J. Lim, A. Tsun, Y. van Kooyk, and E. Caron.** 2006. Two distinct cytoplasmic regions of the beta2 integrin chain regulate RhoA function during phagocytosis. J. Cell Biol. **172:**1069–1079.
31. **Xu, Y., J. Li, G. D. Ferguson, F. Mercurio, G. Khambatta, L. Morrison, A. Lopez-Girona, L. G. Corral, D. R. Webb, B. L. Bennett, and W. Xie.** 2009. Immunomodulatory drugs reorganize cytoskeleton by modulating Rho GTPases. Blood **114:**338–345.
32. **Yu, Y., R. Anjum, K. Kubota, J. Rush, J. Villen, and S. P. Gygi.** 2009. A site-specific, multiplexed kinase activity assay using stable-isotope dilution and high-resolution mass spectrometry. Proc. Natl. Acad. Sci. U. S. A. **106:**11606–11611.

Editor: J. B. Bliska